Magn Reson Med Sci 2018; 17; 42–49
doi:10.2463/mrms.mp.2016-0113
Published Online: May 18, 2017

MAJOR PAPER

Differentiating between Central Nervous System Lymphoma and High-grade Glioma Using Dynamic Susceptibility Contrast and Dynamic Contrast-enhanced MR Imaging with Histogram Analysis

Kazuhiro Murayama[1*], Yuya Nishiyama[2], Yuichi Hirose[2], Masato Abe[3], Shigeharu Ohyu[4], Ayako Ninomiya[4], Takashi Fukuba[5], Kazuhiro Katada[6], and Hiroshi Toyama[1]

Purpose: We evaluated the diagnostic performance of histogram analysis of data from a combination of dynamic susceptibility contrast (DSC)-MRI and dynamic contrast-enhanced (DCE)-MRI for quantitative differentiation between central nervous system lymphoma (CNSL) and high-grade glioma (HGG), with the aim of identifying useful perfusion parameters as objective radiological markers for differentiating between them.

Methods: Eight lesions with CNSLs and 15 with HGGs who underwent MRI examination, including DCE and DSC-MRI, were enrolled in our retrospective study. DSC-MRI provides a corrected cerebral blood volume (cCBV), and DCE-MRI provides a volume transfer coefficient (K^{trans}) for transfer from plasma to the extravascular extracellular space. K^{trans} and cCBV were measured from a round region-of-interest in the slice of maximum size on the contrast-enhanced lesion. The differences in *t* values between CNSL and HGG for determining the most appropriate percentile of K^{trans} and cCBV were investigated. The differences in K^{trans}, cCBV, and K^{trans}/cCBV between CNSL and HGG were investigated using histogram analysis. Receiver operating characteristic (ROC) analysis of K^{trans}, cCBV, and K^{trans}/cCBV ratio was performed.

Results: The 30th percentile (C30) in K^{trans} and 80th percentile (C80) in cCBV were the most appropriate percentiles for distinguishing between CNSL and HGG from the differences in *t* values. CNSL showed significantly lower C80 cCBV, significantly higher C30 K^{trans}, and significantly higher C30 K^{trans}/C80 cCBV than those of HGG. In ROC analysis, C30 K^{trans}/C80 cCBV had the best discriminative value for differentiating between CNSL and HGG as compared to C30 K^{trans} or C80 cCBV.

Conclusion: The combination of K^{trans} by DCE-MRI and cCBV by DSC-MRI was found to reveal the characteristics of vascularity and permeability of a lesion more precisely than either K^{trans} or cCBV alone. Histogram analysis of these vascular microenvironments enabled quantitative differentiation between CNSL and HGG.

Keywords: *central nervous system lymphoma, high-grade glioma, dynamic susceptibility contrast and dynamic contrast-enhanced magnetic resonance imaging, histogram analysis*

Introduction

Differentiation between central nervous system lymphoma (CNSL) and high-grade glioma (HGG) is sometimes difficult because these lesions have similar MRI findings and contrast-enhanced patterns. One difference is that CNSL exhibits lower diffusion, reflecting higher cell density.[1,2] However, in reality, this difference is not very helpful for differentiating between CNSL and HGG, because diffusion is also reduced in many cases of HGG. A more useful difference is in their responses to contrast, with glioblastoma showing a thick, irregular ring-shaped enhancement effect whereas lymphoma appears uniform in regions contacting the cerebrospinal fluid space. The therapeutic strategies of surgery and chemotherapy differ entirely between

[1]Department of Radiology, Fujita Health University, 1-98 Dengakugakubo, Kutsukake-cho Toyoake, Aichi 470-1101, Japan
[2]Department of Neurosurgery, Fujita Health University, Aichi, Japan
[3]Department of Pathology, School of Health Sciences, Fujita Health University, Aichi, Japan
[4]Toshiba Medical Systems Corporation, Tochigi, JAPAN
[5]Department of Radiology, Fujita Health University Hospital, Aichi, Japan
[6]Joint Research Laboratory of Advanced Medical Imaging, Fujita Health University, Aichi, Japan
*Corresponding author, Phone: +81-562-93-9259, Fax: +81-562-95-2253, E-mail: kmura@fujita-hu.ac.jp

Meeting Presentation: This work was presented at the 43rd Japanese Society for Magnetic Resonance in Medicine in Tokyo, 2015.

Received: October 5, 2016 | Accepted: March 29, 2017

HGG and CNSL. While total resection is the usual treatment for glioma, such a large craniotomy is unnecessary for CNSL because only a biopsy is needed. Lymphoma is typically treated with large quantities of methotrexate, whereas malignant glioma is treated with the oral alkylating agent temozolamide. Additionally, an antineoplastic agent for intracerebral implantation has been approved exclusively for the treatment of HGG, further increasing the need for accurate preoperative differentiation between HGG and CNSL.

In addition to morphological diagnosis, perfusion imaging has been used in the differential diagnosis of brain tumors. MRI-based contrast-enhanced perfusion imaging procedures are of two major classes: dynamic contrast-enhanced (DCE)-MRI and dynamic susceptibility contrast (DSC)-MRI. In DSC-MRI, a series of images of the same site is acquired while a contrast agent is administered via intravenous bolus; the microscopic dynamics of regional cerebral blood flow at the capillary level are analyzed and visualized from the resultant time–intensity curve. The DSC-MRI parameter of cerebral blood volume (CBV) is reported to be useful for distinguishing between malignant gliomas and CNSL;[3–5] primary CNSL has lower CBV ratios than does glioblastoma.[3] DCE-MRI visualizes the extravascular permeability of the contrast agent caused by disruption of the blood–brain barrier (BBB). DCE-MRI provides a volume transfer coefficient (K^{trans}) for transfer from plasma to the extravascular extracellular space. At present, various medical image-processing workstations are available to facilitate the creation of these perfusion images and analysis of histograms, making it easier to use these procedures for clinical purposes. Permeability imaging can reveal BBB disturbances and angiogenesis. Relevant reported findings have shown that high-activity portions of a brain tumor have high values;[6,7] primary CNSL demonstrated significantly higher K^{trans} and flux rate constant values compared with glioblastoma.[8]

From these preliminary findings that CBV and K^{trans} differ between CNSL and HGG, we hypothesized that more accurate differentiation might result from evaluating K^{trans}/CBV, which includes both CBV and K^{trans} values. The combined use of DSC-MRI and DCE-MRI is expected to differentiate brain tumors with improved accuracy over the independent use of either one. However, the reported levels of accuracy vary,[3,8] and no established method is available for quantitative differentiation of brain tumors using histograms obtained from the combined use of the two techniques. In this study, we evaluate the diagnostic performance of histogram analysis using a combination of DSC-MRI and DCE-MRI for quantitative differentiation between CNSL and HGG, with the aim of identifying useful objective radiological markers for such differentiating between these two conditions.

Materials and Methods

Subjects

This retrospective study was approved by our institutional review board. 19 preoperative initial patients, 3 postoperative patients with suspected recurrence of HGG, and 1 postoperative patient of CNSL (after biopsy) who underwent DCE and DSC-MRI, using a 3T MRI unit (Vantage Titan 3T with Saturn Gradient Option; Toshiba Medical Systems Corporation, Otawara, Japan) obtained from 23 consecutive patients with suspected or diagnosed CNSL and HGG were enrolled from January 2015 to February 2016. Image from 1 patient was excluded in 3 postoperative patients with suspected recurrence of HGG because the pathological finding showed only reactive therapeutic changes in HGG. The final cohort included 22 patients (11 men and 11 women; age range, 7–86 years; mean age, 59.8 years). Of the enrolled patients, 8 patients had CNSL and 14 patients had HGG as diagnosed based on histopathologic findings. As one patient with HGG had two lesions, 8 CNSL lesions and 15 HGG (grade III, 4 gliomas; grade IV, 11 gliomas) lesions were finally analyzed.

MRI protocol

MRI studies were acquired during routine clinical work-up using a 3T MRI system with a 32-channel head coil for all patients. Axial DCE-MR imaging was performed after intravenous administration of a contrast agent using a 3D fast field echo (FFE) quick sequence that provided coverage of the entire brain tumor using the following parameters: matrix size, zero-filling matrix 512 × 512 (acquisition matrix 186 × 256); FOV, 220 × 220 mm; TR, 5.5 ms; TE, 2.5 ms; flip angle, 15°; section thickness, 5 mm. Thirty-one dynamic consecutive volumes, each including 21 sections to cover the tumor based on T_2-weighted images, were obtained every 10 seconds, giving a total measurement time of 5 minutes, 4 seconds. The contrast agent meglumine gadopentetate (0.05 mmol/kg body weight) (Magnevist; Bayer, Osaka, Japan) or gadoteridol (ProHance; Bracco/Eisai, Tokyo, Japan) was injected intravenously as a bolus through a driven autoinjector (Sonic Shot GX; Nemoto, Japan) at a rate of 1 mL/s, followed by an intravenous bolus injection of 30 mL of physiological saline solution at 1 mL/s.

After completion of the DCE-MR imaging sequence, axial DSC-MR imaging was performed after the intravenous administration of contrast agent with field echo-echo planar T_2^*-weighted imaging providing coverage of the entire brain tumor using the following parameters: matrix size, zero-filling matrix 256 × 256 (acquisition matrix 96 × 128); FOV, 220 × 220 mm; TR, 2000 ms; TE, 25 ms; flip angle, 90°; section thickness, 5 mm. Forty-five dynamic consecutive volumes, each including 17 sections to cover the tumor on the basis of T_2-weighted images, were obtained every 2 seconds, giving a total measurement time of 90 seconds. The above-mentioned contrast agent (0.05 mmol/

kg body weight) was injected intravenously as a bolus through a driven autoinjector at a rate of 3 mL/s, followed by an intravenous bolus injection of 30 mL of physiological saline solution at 3 mL/s. Administration of contrast material for DCE before DSC is known to minimize T_1 effects on CBV measurements.[9]

After completion of the DCE-MR imaging sequence, standard post-contrast 3D FFE data were acquired using the following parameters: matrix size, 256 × 256; FOV, 250 × 250 mm; thickness, 1 mm; 180 sections; TR, 7.9 ms; TE, 3.7 ms; flip angle, 20°; section thickness, 1 mm; number of excitations, 2.

Image postprocessing

Post-processing of DCE and DSC perfusion MR images was performed using dedicated post-processing software (Olea Sphere V3.0, Olea Medical, Vitrea Workstation V7.1, Toshiba Medical Systems Corporation). Motion correction was performed on the dynamic images. On the basis of the 2-compartment pharmacokinetic model proposed by the extended model of Tofts et al.[10] for DCE-MRI, we used the perfusion analysis method to calculate permeability parameter[11] as only K^{trans}. DSC perfusion images were used in the production of CBV maps, with leakage correction (corrected CBV [cCBV]) by use of established tracer kinetic models applied to the first-pass data. Signal intensity was then converted to gadolinium agent concentration, and the time–concentration curve was generated. Automated arterial input function detection was used for calculation. The CBV maps were generated from the time-concentration curve of tissue and artery. In our study, the contrast agent used in DCE-MRI served the same function as the pre-administered contrast agent in preload-leakage correction. In addition, the mathematical correction was performed using the post-processing software. The cCBV and K^{trans} maps were automatically generated based on the pixel information.

Data analysis

After obtaining a kinetic modeling parameter map, a neuroradiologist (K.M.; 14 years of experience) manually placed a round or oval ROI including the maximum contrast-enhanced lesion on the contrast-enhanced T_1WI (Figs. 1, 2). All subjects had clearly defined margins with contrast enhancing. Normal vessels were avoided during ROI placement. These ROIs were copied to the corresponding cCBV and K^{trans} maps on the same location of the contrast-enhanced lesion in all objects. Figures 1 and 2 illustrate examples of manually-drawn ROIs within an enhancing tumor in K^{trans} and cCBV maps and contrast-enhanced T_1WI. ROI values in the same tumor location were compared in the histopathological correlation following the study. We performed histogram analysis of ROIs and acquired 5, 10, 20, 30, 40, 50, 60, 70, 80, 90, 95, and 100 percentile values for K^{trans} and cCBV.

Statistical analysis

We ruled out percentiles with no significant difference in unpaired *t*-test between CNSL and HGG in the histogram analysis. Next, we evaluated the data with the greatest differences in *t* values in significantly different percentiles for

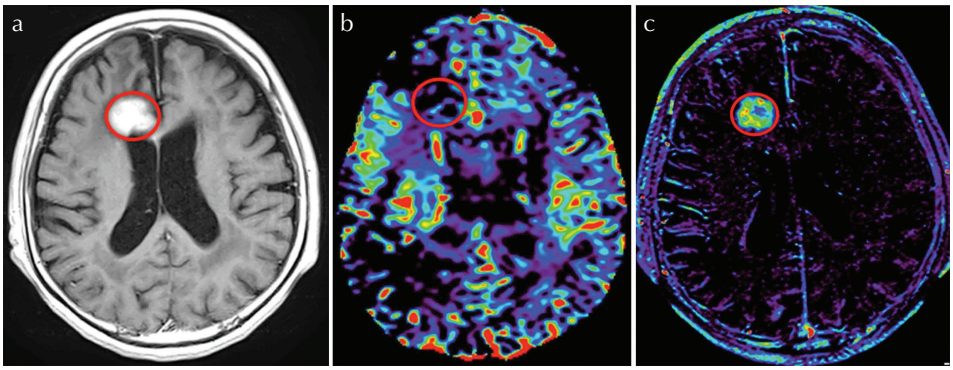

Fig. 1 Contrast-enhanced T_1-weighted images (T_1WI) (**a**), corrected cerebral blood volume (CBV) (**b**), and volume transfer coefficient (K^{trans}) (**c**) in patient with central nervous system lymphoma. Contrast-enhanced T_1WI shows an enhanced mass in the right frontal lobe. Axial corrected CBV shows relatively decreased vascularity, and axial K^{trans} shows increased vascular permeability in the whole lesion.

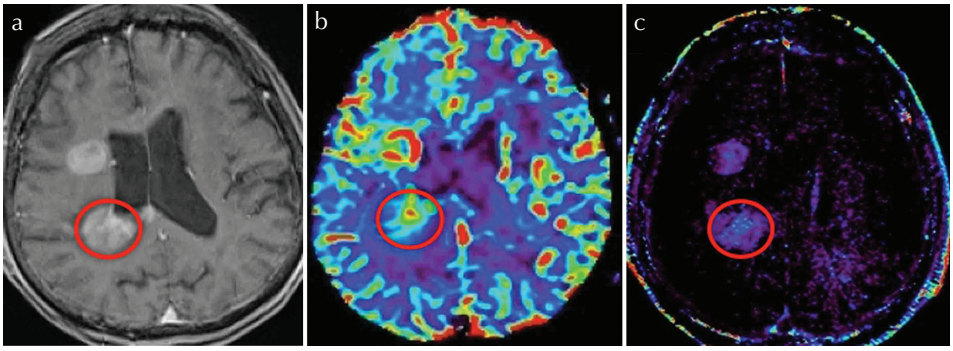

Fig. 2 Contrast-enhanced T_1-weighted images (T_1WI) (**a**), corrected cerebral blood volume (CBV) (**b**), and volume transfer coefficient (K^{trans}) (**c**) in patient with high grade glioma. Contrast-enhanced T_1WI shows an enhanced mass in the right frontal and parietal lobe. Axial corrected CBV shows increased vascularity in the peripheral lesion, and axial K^{trans} shows a small degree of increased vascular permeability.

determining the best percentile of K^{trans} and cCBV to distinguish between these brain tumors. A line graph was drawn to demonstrate the change in *t* values from the 5th to 95th percentiles. The differences in K^{trans}, cCBV, and K^{trans}/cCBV between CNSL and HGG were investigated by histogram analysis. An unpaired *t*-test was used to compare the vascular permeability parameter (K^{trans}) and the perfusion parameter (cCBV) between CNSL and HGG. The percentiles with the highest differences in *t* values were determined for each parameter with the best diagnostic performances. The Mann–Whitney test was used to compare K^{trans}, cCBV, and K^{trans}/cCBV between CNSL and HGG with the best percentile values. A scatter plot was made between the corrected CBV and K^{trans} with the best percentile. Receiver operating characteristic (ROC) analysis of cCBV, K^{trans}, and K^{trans}/cCBV was performed. ROC curves were generated to determine the optimum thresholds for discrimination between CNSL and HGG. The area under the curve (AUC) obtained from ROC analysis was analyzed. $P \leq 0.05$ was considered statistically significant. The cutoff values and the highest AUC with the highest sensitivity and specificity were chosen for each perfusion parameter. For all statistical analyses, a 2-tailed $P \leq 0.05$ was considered statistically significant. Statistical analysis was performed using commercially available statistical software (GraphPad PRISM, version 6; GraphPad Software, San Diego, CA, USA).

Results

The mean K^{trans} and cCBV in each percentile of CNSL and HGG are shown in Fig. 3. The 30th percentile (C30) in K^{trans} and 80th percentile (C80) in cCBV were the most different mean values in each parameter for differentiating.

Quantitative comparisons of the DSC and DCE-MRI parameters between CNSL and HGG are shown in Table 1 and Fig. 4. C30 K^{trans}, C80 cCBV, and C30 K^{trans}/C80 cCBV values were 0.09 ± 0.04/min, 2.72 ± 2.27 mL/100 mL, and 0.04 ± 0.03, respectively, for CNSL and 0.03 ± 0.05 /min, 7.66 ± 4.16 mL/100 mL, and 0.005 ± 0.01, respectively, for HGG. CNSL had a significantly lower C80 cCBV ($P = 0.0025$), significantly higher C30 K^{trans} ($P = 0.0025$), and significantly higher C30 K^{trans}/C80 cCBV ($P < 0.0001$) than did HGG. Scatter plots of these values showed that higher C30 K^{trans} and lower C80 cCBV indicated CNSL (Fig. 5).

The results of the ROC analysis for C30 K^{trans} and C80 cCBV are summarized in Table 2 and Fig. 6. C30 K^{trans}/C80 cCBV had the best discriminative value for differentiating between CNSL and HGG (AUC, 0.958; cutoff value, 0.015; sensitivity, 93.33%; specificity, 87.5%) compared with that of C30 K^{trans} (AUC, 0.875; cutoff value, 0.066; sensitivity, 86.67%; specificity, 87.5%) or C80 cCBV (AUC, 0.875; cutoff value, 3.701; sensitivity, 86.67%; specificity, 87.5%). There were no significant differences in the AUC between C30 K^{trans} and C80 cCBV ($P = 1.00$), C30 K^{trans} and C30 K^{trans}/C80 cCBV ($P = 0.137$), and C80 cCBV and C30 K^{trans}/C80 cCBV ($P = 0.288$).

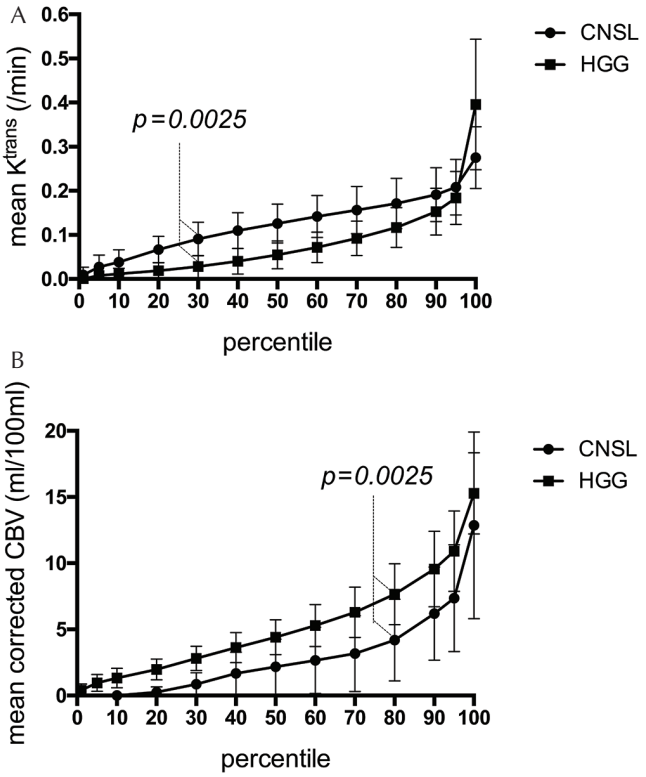

Fig. 3 Mean volume transfer coefficient (K^{trans}) (**A**) and corrected cerebral blood volume (CBV) (**B**) in each percentile. The 30th percentile (C30) in K^{trans} and 80th percentile (C80) in cCBV were the most different mean values in each parameter for differentiating. CNSL, central nervous system lymphoma; HGG, high grade glioma.

Table 1. Quantitative comparison of 30th percentile volume transfer coefficient, 80th percentile corrected cerebral blood volume, and 30th percentile volume transfer coefficient/80th percentile corrected cerebral blood volume between central nervous system lymphoma and high grade glioma

	C30 K^{trans} (/min)		C80 cCBV (ml/100ml)		C30 K^{trans}/C80 cCBV	
CNSL	0.09 ± 0.04	$P = 0.0025$	2.72 ± 2.27	$P = 0.0025$	0.04 ± 0.03	$P < 0.0001$
HGG	0.03 ± 0.05		7.66 ± 4.16		0.005 ± 0.01	

K^{trans}, volume transfer coefficient; cCBV, corrected cerebral blood volume; C30, 30th percentile; C80, 80th percentile; CNSL, central nervous system lymphoma; HGG, high grade glioma.

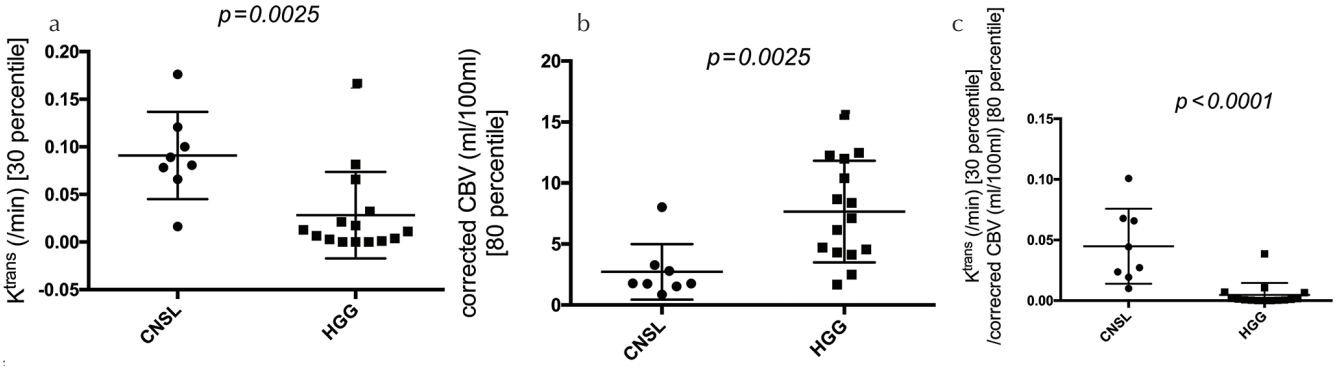

Fig. 4 Quantitative comparisons of the dynamic susceptibility contrast and dynamic contrast-enhanced MRI parameters. (**a**) volume transfer coefficient (K^{trans}), (**b**) corrected cerebral blood volume (CBV), and (**c**) 30th percentile (C30) K^{trans}/80th percentile (C80) corrected CBV. central nervous system lymphoma (CNSL) showed significantly lower C80 corrected CBV, significantly higher C30 K^{trans}, and significantly higher C30 K^{trans}/C80 corrected CBV than those of high-grade glioma (HGG).

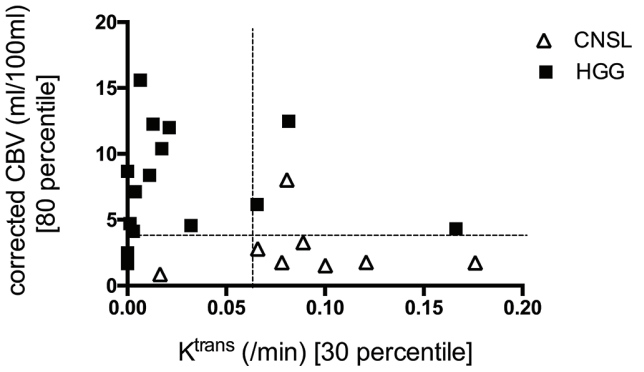

Fig. 5 Scatter plot showing values of corrected cerebral blood volume (CBV) and volume transfer coefficient (K^{trans}). central nervous system lymphoma (CNSL) demonstrates higher K^{trans} and lower corrected CBV than those of high-grade glioma (HGG). The dotted line shows the cutoff value of corrected CBV and K^{trans}.

Representative cases of CNSL and HGG are shown in Figs. 1 and 2. The CNSL example demonstrates a contrast-enhanced lesion in the right frontal white matter (Fig. 1) with decreased cCBV and increased K^{trans}. In contrast, the HGG example demonstrates a contrast-enhanced lesion in the right temporal white matter (Fig. 2) with increased cCBV and a small increase in K^{trans}. These MR perfusion patterns differed considerably.

Discussion

The results of this study indicate that a combination of K^{trans} and cCBV would be useful for differentiating between CNSL and HGG. These parameters have been successfully applied to obtain quantitative estimates of the vascularity and permeability of brain tumors for characterization of the vascular microenvironment.

Histogram analysis is a quantitative technique used in a number of neuroimaging studies on brain tumor differentiation.[12–14] Law et al.[12] reported that CBV histogram analysis was as effective as ROI analysis for determining correlations with glioma grade. Because an evaluation of the partial malignant area in the lesion is difficult using mean ROI analysis in this way, histogram analysis is better for the evaluation of brain tumors. Kim et al.[14] reported that a cumulative histogram analysis of normalized CBV can be a useful method for preoperative glioma grading and that the 99th percentile of the cumulative normalized CBV histogram value was helpful. However, the percentiles of the histogram vary, and the differentiation accuracy and threshold of the MR perfusion image vary between the percentiles used. Jung et al.[15] reported that the 98th percentile value of K^{trans} was the most significant measure. Because the optimal percentile changes depending on the perfusion parameter and evaluation subject, the optimal percentile must be reviewed each time. Because C30 K^{trans} and C80 cCBV were the optimal parameters for the differentiation of CNSL and HGG in our study, we decided to use these percentiles.

CBV calculated by DSC-MRI is known to indicate a tumor vascular bed. Toh et al.[3] reported that primary CNSLs demonstrated significantly lower CBVs than did glioblastomas. In this study, the CBV of CNSL was lower than that of HGG, a finding that is in agreement with those reported in the literature.[16,17] The likely reasons underlying this finding in CNSL include the small number of newly formed blood vessels[17] and underestimation of CBV due to the high permeability as described below. On the other hand, K^{trans} calculated by DCE-MRI is an index of vascular permeability. DCE-MRI parameters have been successfully applied to obtain quantitative estimates of the permeability of brain tumors for characterization of the vascular microenvironment. Kickingereder et al.[8] reported that CNSL demonstrated significantly higher K^{trans}, which indicated a higher vascular permeability in CNSL. In this study, CNSL K^{trans} values were higher and CBV values lower than those of HGG, a finding that is in agreement with those reported in the literature.[8] K2, which has similar significance as K^{trans}, is reported to be associated with the extent of BBB disruption,[3] thus, the observed higher K^{trans} of CNSL likely reflects greater BBB disruption in CNSL than in HGG. However, there are some overlaps in evaluations

Table 2. Receiver operating characteristic analysis of volume transfer coefficient, corrected cerebral blood volume and volume transfer coefficient/corrected cerebral blood volume for differentiation between central nervous system lymphoma and high grade glioma

Parameter	Sensitivity (%)	Specificity (%)	AUC	95% CI	Cutoff value
C30 K^{trans}	86.67	87.5	0.875	0.7273 to 1.023	0.066
C80 cCBV	86.67	87.5	0.875	0.7214 to 1.029	3.701
C30 K^{trans}/ C80 cCBV	93.33	87.5	0.958	0.8820 to 1.035	0.015

K^{trans}, volume transfer coefficient; cCBV, corrected cerebral blood volume; C30, 30th percentile; C80, 80th percentile; AUC, area under the curve; CI, confidence interval.

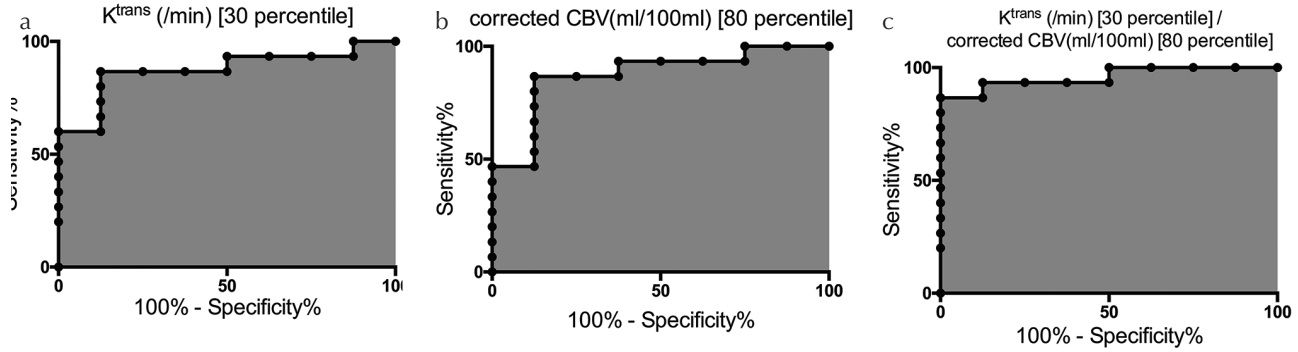

Fig. 6 Receiver operating characteristic curve analysis in differentiating central nervous system lymphoma (CNSL) and high-grade glioma (HGG). (**a**) volume transfer coefficient (K^{trans}), (**b**) corrected cerebral blood volume (CBV), and (**c**) 30th percentile (C30) K^{trans}/80th percentile (C80) corrected CBV. C30 K^{trans}/C80 corrected cerebral blood volume (cCBV) had the best discriminative value for differentiating between CNSL and HGG compared with that for C30 K^{trans} or C80 cCBV.

of K^{trans} and cCBV, and differential accuracy is not enough. CNSL clearly shows high K^{trans} and low CBV in a scatter plot, and K^{trans}/cCBV has the least overlap in comparison with that of each isolated parameter. The combination of K^{trans} and cCBV by optimal percentile would be useful for differentiating between CNSL and gliomas based on ROC analysis. The lack of a significant difference in AUC between C30 K^{trans}, C80 cCBV, and K^{trans}/cCBV likely resulted from the small number of subjects in this study cohort.

One problem with the DSC-MRI examination of brain tumors is that CBV is underestimated because of contrast leakage from blood vessels into tissues. There are two known solutions for this problem. One is preload-leakage correction, in which approximately half of the total dose of the contrast agent is administered some time before DSC imaging is performed.[9] The other is the mathematical correction of time–concentration curves.[18] In our study, the subjects underwent DCE-MRI before DSC-MRI, and the contrast agent used in DCE-MRI served the same function as the preadministered contrast agent in preload-leakage correction. In addition, mathematical correction was performed using postprocessing software. We obtained original time–concentration curves by excluding the T_1 component that changed by contrast media leakage, and cCBV maps were calculated.

Time-consuming DCE-MRI examinations are difficult to perform in real-world clinical settings. Abe et al.[19] reported on the usefulness of a short-time imaging method in which both DSC and DCE information can be obtained in a short period of time. Alternatively, K2 obtained in DSC examinations is a coefficient used for leakage correction and can serve as a rough measure of permeability. Published studies have demonstrated that K2 can be used for differentiating between CNSL and HGG[3] and that K2 shows a similar tendency as K^{trans},[20] suggesting that the use of K2 in place of K^{trans} is also a good option when a sufficient length of time cannot be devoted to examinations.

Because the therapeutic strategies for surgery and chemotherapy differ between HGG and CNSL, it is important to differentiate CNSL and HGG preoperatively using MRI findings. Furthermore, the use of 1,3-Bis (2-chloroethyl)-1-nitrosourea wafers (BCNU) on the surface of tumor resection cavities was efficacious for local chemotherapy in patients with recurrent glioblastoma.[21,22] Before using BCNU wafers, HGG must be confirmed intraoperatively through rapid histopathological diagnosis. However, CNSL and HGG are sometimes difficult to differentiate in rapid pathological diagnoses because they can have similar pathological findings. MR perfusion imaging is more objective than morphological imaging and, therefore, better facilitates understanding and sharing of preoperative imaging between not only radiologists but also neurosurgeons and pathologists. Therefore, MR perfusion imaging results are useful as radiological markers in preoperative diagnostic imaging.

This study has several limitations. First, the number of subjects was small in this retrospective analysis. Future

prospective studies should include more subjects. Second, the contrast medium volume was calculated based on the patient's body weight. To obtain both vascularity and permeability information for routine doses of contrast media at the same examination, contrast media (0.05 mmol/kg body weight) was injected as a bolus twice. The results may have depended on the dose and injection rate of the contrast media, so that the accuracy of DSC and DCE analysis in this study may be lower than if one full dose was used. Third, the ROIs were set manually, and it is possible that measurement results were affected to some extent by the location of the chosen ROI. However, histogram analysis is more effective than mean ROI analysis for including vasculature, a lesion with a higher value in a region, or a lesion with a low value caused by necrosis. Fourth, the results may have been affected by the analysis software used for DCE and DSC-MRI.[23] Because the algorithms and devices used for perfusion analysis vary depending on references, a simple comparison between past references may be difficult.

In conclusion, the combination of K^{trans} by DCE-MRI and cCBV by DSC-MRI may reveal the perfusion characteristics of lesions more precisely than can either K^{trans} or cCBV alone. Histogram analysis results of perfusion data to identify objective radiological markers enable quantitative differentiation between CNSL and HGG.

Acknowledgments

This work was supported by a Grant-in-Aid for Scientific Research (No. 16K20028).

Conflicts of Interest

The authors declare that they have no conflicts of interest.

References

1. Okamoto K, Ito J, Ishikawa K, Sakai K, Tokiguchi S. Diffusion-weighted echo-planar MR imaging in differential diagnosis of brain tumors and tumor-like conditions. Eur Radiol 2000; 10:1342–1350.
2. Guo AC, Cummings TJ, Dash RC, Provenzale JM. Lymphomas and high-grade astrocytomas: comparison of water diffusibility and histologic characteristics. Radiology 2002; 224:177–183.
3. Toh CH, Wei KC, Chang CN, Ng SH, Wong HF. Differentiation of primary central nervous system lymphomas and glioblastomas: comparisons of diagnostic performance of dynamic susceptibility contrast-enhanced perfusion MR imaging without and with contrast-leakage correction. AJNR Am J Neuroradiol 2013; 34:1145–1149.
4. Calli C, Kitis O, Yunten N, Yurtseven T, Islekel S, Akalin T. Perfusion and diffusion MR imaging in enhancing malignant cerebral tumors. Eur J Radiol 2006; 58: 394–403.
5. Hartmann M, Heiland S, Harting I, et al. Distinguishing of primary cerebral lymphoma from high-grade glioma with perfusion-weighted magnetic resonance imaging. Neurosci Lett 2003; 338:119–122.
6. Hoeffner EG, Case I, Jain R, et al. Cerebral perfusion CT: technique and clinical applications. Radiology 2004; 231:632–644.
7. Roberts HC, Roberts TP, Lee TY, Dillon WP. Dynamic, contrast-enhanced CT of human brain tumors: quantitative assessment of blood volume, blood flow, and microvascular permeability: report of two cases. AJNR Am J Neuroradiol 2002; 23:828–832.
8. Kickingereder P, Sahm F, Wiestler B, et al. Evaluation of microvascular permeability with dynamic contrast-enhanced MRI for the differentiation of primary CNS lymphoma and glioblastoma: radiologic-pathologic correlation. AJNR Am J Neuroradiol 2014; 35:1503–1508.
9. Hu LS, Baxter LC, Pinnaduwage DS, et al. Optimized preload leakage-correction methods to improve the diagnostic accuracy of dynamic susceptibility-weighted contrast-enhanced perfusion MR imaging in posttreatment gliomas. AJNR Am J Neuroradiol 2010; 31:40–48.
10. Tofts PS, Brix G, Buckley DL, et al. Estimating kinetic parameters from dynamic contrast-enhanced T(1)-weighted MRI of a diffusable tracer: standardized quantities and symbols. J Magn Reson Imaging 1999; 10:223–232.
11. Tofts PS, Kermode AG. Measurement of the blood-brain barrier permeability and leakage space using dynamic MR imaging. 1. Fundamental concepts. Magn Reson Med 1991; 17:357–367.
12. Law M, Young R, Babb J, Pollack E, Johnson G. Histogram analysis versus region of interest analysis of dynamic susceptibility contrast perfusion MR imaging data in the grading of cerebral gliomas. AJNR Am J Neuroradiol 2007; 28:761–766.
13. Kang Y, Choi SH, Kim YJ, et al. Gliomas: Histogram analysis of apparent diffusion coefficient maps with standard- or high-b-value diffusion-weighted MR imaging—correlation with tumor grade. Radiology 2011; 261:882–890.
14. Kim H, Choi SH, Kim JH, et al. Gliomas: Application of cumulative histogram analysis of normalized cerebral blood volume on 3 T MRI to tumor grading. PLoS ONE 2013; 8:e63462.
15. Jung SC, Yeom JA, Kim JH, et al. Glioma: application of histogram analysis of pharmacokinetic parameters from T_1-weighted dynamic contrast-enhanced MR imaging to tumor grading. AJNR Am J Neuroradiol 2014; 35:1103–1110.
16. Cho SK, Na DG, Ryoo JW, et al. Perfusion MR imaging: clinical utility for the differential diagnosis of various brain tumors. Korean J Radiol 2002; 3:171–179.
17. Liao W, Liu Y, Wang X, et al. Differentiation of primary central nervous system lymphoma and high-grade glioma with dynamic susceptibility contrast-enhanced perfusion magnetic resonance imaging. Acta Radiol 2009; 50:217–225.
18. Boxerman JL, Schmainda KM, Weisskoff RM. Relative cerebral blood volume maps corrected for contrast agent extravasation significantly correlate with glioma tumor grade, whereas uncorrected maps do not. AJNR Am J Neuroradiol 2006; 27:859–867.

19. Abe T, Mizobuchi Y, Nakajima K, et al. Diagnosis of brain tumors using dynamic contrast-enhanced perfusion imaging with a short acquisition time. Springerplus 2015; 4:88.
20. Taoka T, Kawai H, Nakane T, et al. Application of histogram analysis for the evaluation of vascular permeability in glioma by the K2 parameter obtained with the dynamic susceptibility contrast method: Comparisons with Ktrans obtained with the dynamic contrast enhance method and cerebral blood volume. Magn Reson Imaging 2016; 34:896–901.
21. Brem H, Piantadosi S, Burger PC, et al. Placebo-controlled trial of safety and efficacy of intraoperative controlled delivery by biodegradable polymers of chemotherapy for recurrent gliomas. Lancet 1995; 22:1008–1012.
22. Westphal M, Hilt DC, Bortey E, et al. A phase 3 trial of local chemotherapy with biodegradable carmustine (BCNU) wafers (Gliadel wafers) in patients with primary malignant glioma. Neuro Oncol 2003; 5:79–88.
23. Kudo K, Uwano I, Hirai T, et al. Comparison of different post-processing algorithms for dynamic susceptibility contrast perfusion imaging of cerebral gliomas. Magn Reson Med Sci 2017; 16:129–136.